

# Evolution of surface morphology and photoluminescence characteristics of 1.3- $\mu\text{m}$ $\text{In}_{0.5}\text{Ga}_{0.5}\text{As}/\text{GaAs}$ quantum dots grown by molecular beam epitaxy

Quanxiang Wei (魏全香)<sup>1\*</sup>, Zhengwei Ren (任正伟)<sup>2</sup>, Zhenhong He (贺振宏)<sup>2</sup>, and Zhichuan Niu (牛智川)<sup>2</sup>

<sup>1</sup>Department of Physics, Shanxi University, Taiyuan 030006

<sup>2</sup>Institute of Semiconductors, Chinese Academy of Sciences, Beijing 100083

\*E-mail: qx.wei@163.com

Received February 28, 2008

Evolution of surface morphology and optical characteristics of 1.3- $\mu\text{m}$   $\text{In}_{0.5}\text{Ga}_{0.5}\text{As}/\text{GaAs}$  quantum dots (QDs) grown by molecular beam epitaxy (MBE) are investigated by atomic force microscopy (AFM) and photoluminescence (PL). After deposition of 16 monolayers (ML) of  $\text{In}_{0.5}\text{Ga}_{0.5}\text{As}$ , QDs are formed and elongated along the  $[1\bar{1}0]$  direction when using sub-ML depositions, while large size  $\text{InGaAs}$  QDs with better uniformity are formed when using ML or super-ML depositions. It is also found that the larger size QDs show enhanced PL efficiency without optical nonlinearity, which is in contrast to the elongated QDs.

OCIS codes: 160.6000, 250.5230, 310.1860.

doi: 10.3788/COL20090701.0052.

In recent years, there is a continuing interest in self-organized  $\text{In}(\text{Ga})\text{As}/\text{GaAs}$  quantum dots (QDs) structure, because it has been recognized as a new candidate for potential applications in high performance semiconductor lasers emitting at the wavelengths of 1.3 – 1.55  $\mu\text{m}$ <sup>[1–6]</sup>. In general,  $\text{In}(\text{Ga})\text{As}/\text{GaAs}$  QDs are expected to have more advanced optical performance and cheaper in technology than that of 1.3- $\mu\text{m}$   $\text{InP}$  based lasers. However, in  $\text{In}(\text{Ga})\text{As}/\text{GaAs}$  heteroepitaxial systems, elastic strain arising from the lattice mismatch greatly influences the growth and microstructure of the over layer. As a result, many aspects concerning size, shape, and composition fluctuations of the QDs are still not understood extensively. Whether the strain can be released efficiently decides the composition and the size distribution of three-dimensional (3D) QDs. Thus, it is very necessary to study the surface morphology evolution of 1.3- $\mu\text{m}$  emission  $\text{In}(\text{Ga})\text{As}/\text{GaAs}$  QDs which can result directly from the strain relaxation mechanism of the deposited  $\text{InGaAs}$  layer.

It is well known that low growth rate, alternate supply growth, and  $\text{InGaAs}$  strain-reducing layer are the keys to attain 1.3- $\mu\text{m}$  emission in  $\text{In}(\text{Ga})\text{As}/\text{GaAs}$  QDs<sup>[7–11]</sup>. But increasing the amount of deposited  $\text{In}(\text{Ga})\text{As}$  is found to be another important factor. For example, it needs ten or more monolayers (ML)  $\text{InGaAs}$  QDs for the 1.3- $\mu\text{m}$  photoluminescence (PL) emission<sup>[1]</sup>. Recently, we found that by depositing 16 ML  $\text{InGaAs}$  via cycled ML  $(\text{InAs})_1/(\text{GaAs})_1$  deposition, the formed island can reach a room temperature  $\sim 1.35\text{-}\mu\text{m}$  PL with good optical properties<sup>[3]</sup>.

In this letter, we report a systematic investigation of the morphological evolution and optical properties of molecular beam epitaxy (MBE)-grown  $\text{In}_{0.5}\text{Ga}_{0.5}\text{As}/\text{GaAs}$  QDs via cycled  $(\text{InAs})_n/(\text{GaAs})_n$  ML deposition method, where  $n$  stands for the number of the deposited ML ranging from 0.0 to 2.0 ( $n < 1$ , sub-ML;  $n = 1$ , ML,  $n > 1$ , super-ML, respectively).

It is demonstrated, from the atomic force microscopy (AFM) results, that the style of the deposition can directly control the surface morphology of the deposited  $\text{InGaAs}$  layer. Therefore, it is possible to obtain strain released 1.3- $\mu\text{m}$  emission  $\text{InGaAs}$  QDs or highly strained QDs via cycled  $(\text{InAs})_n/(\text{GaAs})_n$  ML deposition.

Samples studied here were grown in a VG V80H MKII MBE system on (100) semi-insulating  $\text{GaAs}$  substrates. A first 500-nm  $\text{GaAs}$  buffer layer was grown at a substrate temperature of 600 °C. Then the growth was interrupted in order to reduce the substrate temperature to 510 °C, which was then kept constant for the growth of the rest layers. The 16 ML  $\text{In}_{0.5}\text{Ga}_{0.5}\text{As}$  QDs were formed by alternatively growing  $n$  ML  $\text{InAs}$  and  $n$  ML  $\text{GaAs}$ , where  $n = 0.25, 0.5, 1.0, 1.5$ , and 2.0. For all samples, 30-seconds  $\text{As}_4$  exposure pause was introduced between each cycled  $\text{InAs}$  and  $\text{GaAs}$  layer. In order to carry out AFM measurements, after the  $\text{In}_{0.5}\text{Ga}_{0.5}\text{As}$  island deposition, the samples were quickly cooled to 300 °C, while the arsenic pressure was maintained to reduce surface reorganization. For samples designed for PL measurement, the  $\text{In}_{0.5}\text{Ga}_{0.5}\text{As}$  QDs were covered by overgrowth layers including a 3 ML Indium-segregation-suppressing  $\text{AlAs}$  layer, a 3-nm strain-reducing  $\text{In}_{0.2}\text{Ga}_{0.8}\text{As}$  layer and finally a 50-nm  $\text{GaAs}$  cap layer. For comparison, a special 16-ML-thick  $\text{In}_{0.5}\text{Ga}_{0.5}\text{As}$  island structure (nominated as  $n = 0.0$  sample) was grown with  $\text{In}$  and  $\text{Ga}$  sources supplied simultaneously, also sandwiched by the same buffer and overgrowth layers as above for PL measurement. The growth rates of  $\text{InAs}$  and  $\text{GaAs}$  were 0.1 and 0.5 ML/s calibrated by reflection high-energy electron diffraction (RHEED) intensity oscillations. The back pressure of  $\text{As}_4$  was maintained at  $2 \times 10^{-8}$  mbar during the growth.

AFM morphology measurements were carried out using a Park Science Instruments (PSI) microscope, model VP, operating in the contact mode. Images were analyzed using PSI pro scan image processing software,

version 1.5. The He-Ne laser with the wavelength of 632.8 nm was used as an excitation source for the PL measurement. Excitation power and sample temperature were changeable from 0.03 to 30 mW and from 10 to 300 K, respectively. A liquid nitrogen cooled Ge detector detected the PL signals from the samples.

Figures 1(a)–(f) show typical AFM images of all the samples with their height profiles. Besides the flat areas corresponding to the wetting layer, the surface of the  $n = 0.0$  sample (Fig. 1(a)) consists of QDs with a lateral size of 80 nm and a height of about 10 nm. When the InGaAs QDs are formed via cycled  $(\text{InAs})_n/(\text{GaAs})_n$  deposition ( $n > 0.0$ ), their shapes, sizes, and lateral distributions are quite different depending on the ML number  $n$ . For  $n = 0.25$ , QDs as shown in Fig. 1(b) are elongated along the  $[1\bar{1}0]$  direction with a bigger size and smaller density than those of the  $n = 0.0$  sample. With increasing ML number to  $n = 0.5$ , coalescence of the elongated QDs occurs, resulting a ripple morphology. However, for  $n = 1.0$ , the elongated QDs coalesce with each other only in the  $[1\bar{1}0]$  direction whereas a quite uniform periodicity of about 90 nm along the  $[110]$  direction can be recognized as shown by Fig. 1(d), which can be referred to as mounds structure. Further increasing ML number  $n$  to 1.5, the deposited InGaAs materials nucleate to QDs again, but the QDs are still elongated slightly along the

$[1\bar{1}0]$  direction, especially for the QDs with a smaller lateral size along the  $[110]$  direction. Finally, when  $n = 2.0$ , uniform QDs, which have an average lateral size of 95 nm and a height of about 10 nm, are formed without obvious direction preferential.

We attribute the surface morphology mainly to the lattice mismatch between GaAs and InGaAs with different Indium mole fraction. It is well known that larger In fraction results in larger lattice mismatch between GaAs and InGaAs. When the InGaAs layer is formed via cycled  $(\text{InAs})_n/(\text{GaAs})_n$  ( $n > 0.0$ ) depositions, the mismatch between the first deposited InGaAs layer and the GaAs substrate is smaller for  $n < 1.0$  than for  $n \geq 1.0$ , because In and Ga exist simultaneously in the first  $n < 1.0$  deposition layer while there is only In component in the first  $n \geq 1.0$  deposition layer. Therefore, sub-ML deposition is similar to the  $n = 0.0$  sample case, but for bigger ML number, the deposition mechanism turns to InAs/GaAs case. As a result, when  $n < 1.0$ , because 16 ML exceed the critical thickness of  $\text{In}_{0.5}\text{Ga}_{0.5}\text{As}$ , island saturation occurs and disordered morphology is observed in Fig. 1(a)<sup>[12]</sup>; for  $n = 0.25$  and 0.5, surface adatom diffusion is more sufficient for the QDs to reach the optimal size of lower strain state, so the QDs are elongated along the  $[1\bar{1}0]$  direction, which gives the typical anisotropic surface morphology for As-stabilized surface<sup>[13]</sup>. Particularly, it should be noted that the ripple morphology when  $n = 0.5$  results in large stress state of the QDs, which will be proved in our PL measurements. When  $n \geq 1.0$ , due to the high strain in the first deposited atom layer, preferential sites exist for dots formed in successive InAs layers, also new QDs tend to nucleate directly above buried QDs<sup>[14,15]</sup>, therefore QDs are formed with different size and distribution other than those for  $n < 1.0$ .

PL measurements can give us the information about the stress state of the lattice-mismatched InGaAs/GaAs system. Figure 2(a) shows the PL spectra from the six samples taken at 10 K under constant excitation power of 0.3 mW. The PL peak energy and the full-width at half-maximum (FWHM) of spectra are displayed in Fig. 2(b) for clarity. In Fig. 2(a), the PL signals are quite strong for  $n > 0.0$  samples, while a sharp drop in PL intensity is observed for  $n = 0.0$  sample. For the curve  $n = 1.0$ , besides the main peak at about 1.00 eV (marked as (1)), there is

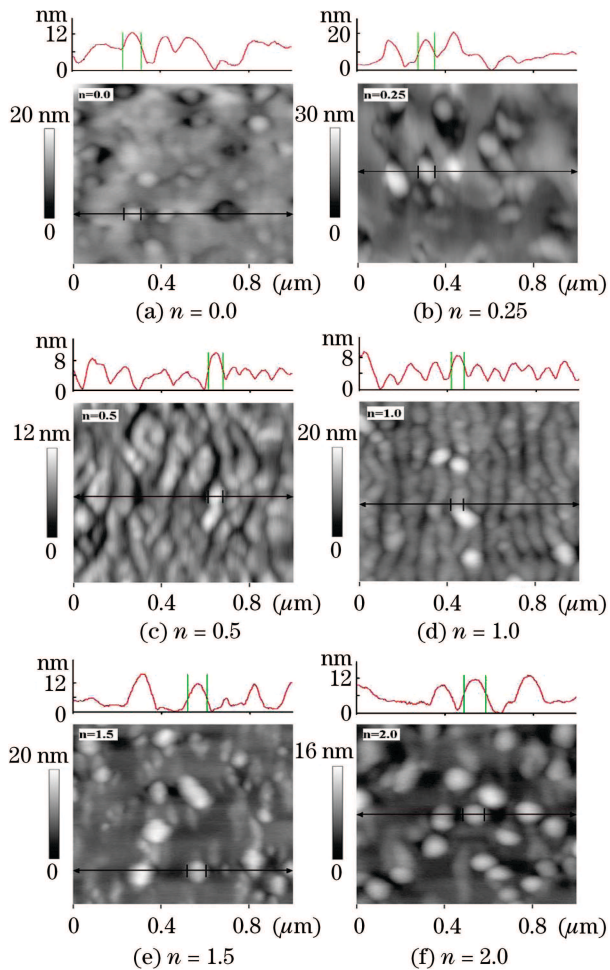


Fig. 1. Typical *ex situ* AFM images of the surface morphologies of the  $\text{In}_{0.5}\text{Ga}_{0.5}\text{As}$  QDs corresponding to the ML number  $n$  from 0.0 to 2.0.

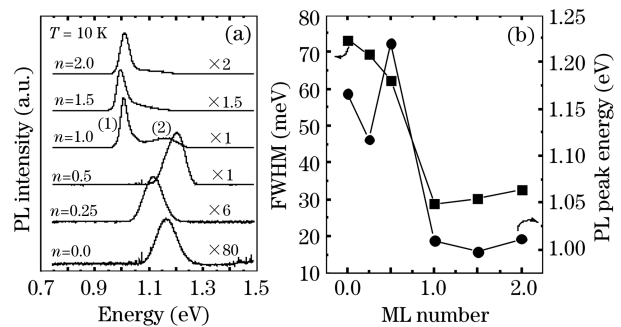


Fig. 2. (a) PL spectra taken at 10 K under excitation power of 0.3 mW for all the cycled  $(\text{InAs})_n/(\text{GaAs})_n$  ( $n = 0.0 - 2.0$ ) grown island samples. The separated higher energy peak of  $n = 1.0$  curve (marked as peak (2)) is positioned at about 1.17 eV; (b) PL peak energy and the FWHM of spectra with different ML number  $n$ .

a fairly separated PL peak at about 1.170 eV (marked as (2)). From Fig. 2(b), it is clear that  $n \geq 1.0$  samples show lower emission energy and narrower FWHM compared to  $n < 1.0$  samples. The lowest PL peak energy obtained here is 0.99 eV from the  $n = 1.5$  island structure, which is 180 meV red-shifted compared to the peak of 1.17 eV from the  $n = 0.0$  sample. In particular, PL peak of the  $n = 0.5$  curve is located at energy position of about 1.22 eV, which is the highest among those PL spectra. For FWHM, the narrowest linewidth of 28.8 meV is obtained from the PL spectra of the  $n = 1.0$  sample. The FWHM of the  $n = 0.0$  sample reaches the maximum value of 73 meV.

It is known that strain relaxation of the InGaAs island greatly influences the energy band structure<sup>[16]</sup>. The higher the stress state, the higher energy it emits. In our case, since the widths of all the samples are the same and they are covered by the same overgrowth layers, so it is easy to conclude that elastic strain of  $n \geq 1.0$  QDs relaxed more than that of  $n < 1.0$  QDs. Thus, the lower stress state of the InGaAs mounds and large size InGaAs QDs of  $n \geq 1.0$  reduces the interband transition energy and thereby increases the energy shift up to 180 meV at 10K compared with the  $n = 0.0$  structure. This conclusion can further be proved by the following optical nonlinearity of the  $n < 1.0$  samples.

The narrower FWHM of the PL of the  $n \geq 1.0$  samples originates from the uniformity of the InGaAs mounds or QDs. Because from AFM images, it can be seen that for  $n = 1.0$ , the lateral width of the mounds along the [110] direction is roughly the same, and the height has a quite small fluctuation. It is also true for the large size QDs formed by the super-ML deposition ( $n > 1.0$ ). However, the surface of the  $n < 1.0$  InGaAs QDs has a bigger width fluctuation, which results in the broader FWHM of the PL spectrum. For the  $n = 0.5$  QDs, the PL peak intensity is the highest of 1.22 eV which may due to the less defects of the  $n = 0.5$  QDs than other QDs. While the two PL features appeared only for the  $n = 1.0$  sample may be attributed to their elongated shapes of the QDs and distributions of carriers at room temperature.

The above observations confirm that the PL performance of the samples correlates to the surface morphologies of the  $\text{In}_{0.5}\text{Ga}_{0.5}\text{As}$  QDs, which play an important role for strain relaxation of the InGaAs QDs. Moreover, the strained QDs should show optical nonlinearity due to internal piezoelectric fields effect, but this effect does not exist in unstrained QDs<sup>[17]</sup>. Evidence has been obtained when we measure the PL peak energy from the ground states of all samples and the separated peak of  $n = 1.0$  sample under different excitation intensities and Fig. 3 shows the results.

In Fig. 3, in contrast to the blueshift of PL peak energy shown by the InGaAs QDs of  $n < 1.0$  when the excitation power is raised, the  $n \geq 1.0$  InGaAs mounds or QDs do not show optical nonlinearity. The  $n = 0.5$  QDs show a strong blueshift up to 0.69 eV for an increase of the excitation power from 0.03 to 30 mW, whereas the peak energies of  $n = 0.25$  and 0.0 sample show appropriately the same value of shift at high excitation power. For samples of  $n \geq 1.0$ , increases of excitation power do not result in the blueshift of PL peak of ground states but a slight redshift that need further investigation. For the

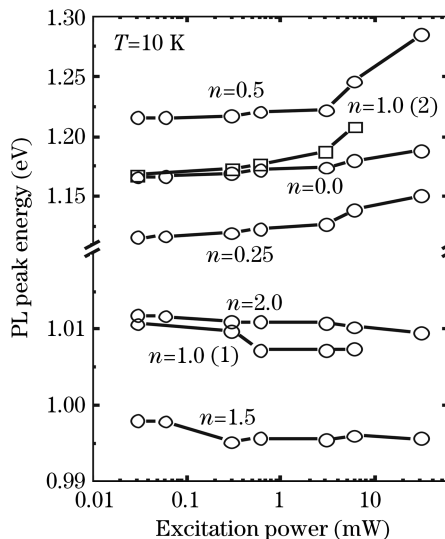


Fig. 3. Spectra of PL energy peak versus excitation power intensity taken at 10 K from all the cycled  $(\text{InAs})_n/(\text{GaAs})_n$  ( $n = 0.0 - 2.0$ ) grown QDs. For  $n = 1.0$ , the peak change of ground state is marked as (1), and the separated peak marked as (2).

separated peak marked (2) of  $n = 1.0$  sample, it shows a similar blueshift as the  $n = 0.5$  sample with the excitation power.

The strongest optical nonlinearity shown by the  $n = 0.5$  sample suggests that large strain exists in the InGaAs QDs layer. This can be explained by the fact that the InGaAs QDs, which are in contact with each other (Fig. 1(c)), may result in the large stress state of the InGaAs layer. Some features of this remains for the  $n = 1.0$  sample and results in the separated PL peak, which shows a similar optical properties of the  $n = 0.5$  sample. The same energy shift for the  $n = 0.25$  and 0.0 samples suggests that small ML number  $n$  is not suitable for the strain relaxation of the InGaAs layer. However, absence of optical nonlinearity of  $n \geq 1.0$  samples proves that strain relaxation has been achieved through the quite uniform surface morphology of these mounds or QDs. Therefore, from the experiment results, we have obtained a critical value of  $n = 1.0$  for strain released  $1.3\text{-}\mu\text{m}$  emission in InGaAs QDs formation.

Finally, it is necessary to compare the PL efficiency

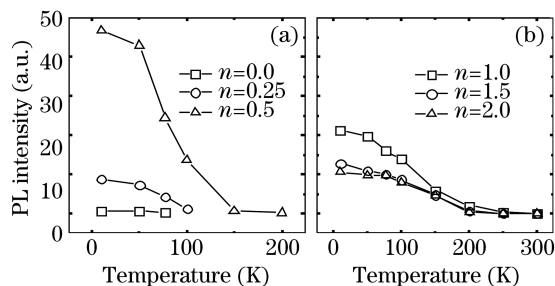


Fig. 4. Comparison of the temperature dependent spectra of PL integrated intensity measured under the constant excitation power of 0.3 mW. (a) No detectable PL emissions from the  $n = 0.0, 0.25$  and  $0.5$  samples, if the temperature is increased above 77, 100 and 200 K, respectively; (b) strong PL signals from samples  $n = 1.0, 1.5$  and  $2.0$  can be detected until the measured temperature about 300 K.

for all samples under different temperatures, as shown in Fig. 4. In Fig. 4(a), no PL signal can be detected at higher temperatures for the  $n < 1.0$  samples, because the PL intensities are very weak even at low temperatures ( $n = 0.0$  and  $0.25$ ) or decrease dramatically with increasing temperature ( $n = 0.5$ ), and the highest temperature at which the PL signal can be detected is 200 K for the  $n = 0.5$  sample. While quite strong PL signals under excitation power of 0.3 mW measured from 10 to 300 K are detectable for all the  $n \geq 1.0$  samples (Fig. 4(b)), and the peak position of the three samples at 300 K is about  $1.35 \mu\text{m}$ . Moreover, for the  $n = 1.0$  sample, the PL intensity is higher than that of the  $n = 1.5$  and  $2.0$  samples at the same temperature. From the measurement results discussed above, the PL efficiencies of the samples grown by ML and super-ML depositions ( $n \geq 1.0$ ) compared to the samples grown by sub-ML depositions ( $n < 1.0$ , including  $n = 0.0$ ) are clearly enhanced as evidenced.

In summary, we have studied the morphology evolution and PL properties of  $\text{In}_{0.5}\text{Ga}_{0.5}\text{As}/\text{GaAs}$  island structures grown by cycled  $(\text{InAs})_n/(\text{GaAs})_n$  deposition method. The strain relaxation of the  $\text{InGaAs}$  QDs achieved through the evolution of surface morphology has been proved by the optical nonlinearity of PL spectra taken from the  $n < 1.0$  QDs under different excitation intensities. The  $n \geq 1.0$  depositions result in efficient strain relaxation of the  $\text{InGaAs}$  layer and enhancement of  $1.3\text{-}\mu\text{m}$  PL efficiency till room temperature.

This work was supported by the National Natural Science Foundation of China (No. 10734060) and the National Basic Research Program of China (No. 2006CB921504).

## References

1. D. L. Huffaker, G. Park, Z. Zou, O. B. Shchekin, and D. G. Deppe, *Appl. Phys. Lett.* **73**, 2564 (1998).
2. K. Mukai, Y. Nakata, K. Otsubo, M. Sugawara, N. Yokoyama, and H. Ishikawa, *IEEE Photon. Technol. Lett.* **11**, 1205 (1999).
3. X. D. Wang, Z. C. Niu, S. L. Feng, and Z. H. Miao, *J. Cryst. Growth* **220**, 16 (2000).
4. V. M. Ustinov, N. A. Maleev, A. E. Zhukov, A. R. Kovsh, A. Yu. Egorov, A. V. Lunev, B. V. Volovik, I. L. Krestnikov, Yu. G. Musikhin, N. A. Bert, P. S. Kop'ev, Zh. I. Alferov, N. N. Ledentsov, and D. Bimberg, *Appl. Phys. Lett.* **74**, 2815 (1999).
5. D. Guimard, S. Tsukamoto, M. Nishioka, and Y. Arakawa, *Appl. Phys. Lett.* **89**, 083116 (2006).
6. Q. Han, Z. Niu, H. Ni, S. Zhang, X. Yang, Y. Du, C. Tong, H. Zhao, Y. Xu, H. Peng, and R. Wu, *Chin. Opt. Lett.* **4**, 413 (2006).
7. K. Mukai, N. Ohtsuka, M. Sugawara, and S. Yamazaki, *Jpn. J. Appl. Phys.* **33**, L1710 (1994).
8. R. P. Mirin, J. P. Ibbetson, K. Nishi, A. C. Gossard, and J. E. Bowers, *Appl. Phys. Lett.* **67**, 3795 (1995).
9. R. Murray, D. Childs, S. Malik, P. Siverns, C. Roberts, J. M. Hartmann, and P. Stavrinou, *Jpn. J. Appl. Phys.* **38**, 528 (1999).
10. M. Arzberger, U. Kasberger, G. Bohm, and G. Abstreiter, *Appl. Phys. Lett.* **75**, 3968 (1999).
11. K. Nishi, H. Saito, S. Sugou, and J.-S. Lee, *Appl. Phys. Lett.* **74**, 1111 (1999).
12. R. Leon and S. Fafard, *Phys. Rev. B* **58**, R1726 (1998).
13. J. Sudijono, M. D. Johnson, C. W. Snyder, M. B. Elowitz, and B. G. Orr, *Phys. Rev. Lett.* **69**, 2811 (1992).
14. J. Tersoff, C. Teichert, and M. G. Lagally, *Phys. Rev. Lett.* **76**, 1675 (1996).
15. X. D. Wang, Z. C. Niu, and S. L. Feng, *Jpn. J. Appl. Phys.* **39**, 5076 (2000).
16. D. J. Arent, K. Deneffe, C. Van Hoof, J. De Boeck, and G. Borghs, *J. Appl. Phys.* **66**, 1739 (1989).
17. M. Grundmann, O. Stier, and D. Bimberg, *Phys. Rev. B* **52**, 11969 (1995).